Thermodynamics of the one-dimensional parallel Kawasaki model: Exact solution and mean-field approximations

Federico G. Pazzona,[*] Pierfranco Demontis, and Giuseppe B. Suffritti
Dipartimento di Chimica e Farmacia, Università degli Studi di Sassari, 07100 Sassari, Italy

The adsorption isotherm for the recently proposed parallel Kawasaki (PK) lattice-gas model [Phys. Rev. E **88**, 062144 (2013)] is calculated exactly in one dimension. To do so, a third-order difference equation for the grand-canonical partition function is derived and solved analytically. In the present version of the PK model, the attraction and repulsion effects between two neighboring particles and between a particle and a neighboring empty site are ruled, respectively, by the dimensionless parameters ϕ and θ. We discuss the inflections induced in the isotherms by situations of high repulsion, the role played by finite lattice sizes in the emergence of substeps, and the adequacy of the two most widely used mean-field approximations in lattice gases, namely, the Bragg-Williams and the Bethe-Peierls approximations.

I. INTRODUCTION

Due to their discreteness, which makes them amenable to theoretical investigations as well as efficient tools in the production of coarse-grained models, lattice gases [1,2] are still widely used in computational physics and chemistry [3–23]. In not-so-recent times, cellular automata (CA) were introduced as highly parallel computational tools in the study of fluids and complex systems on the mesoscopic scale [24–27]. Although CA found a huge number of applications in the field of chemical physics, ranging from hydrodynamics [28] to adsorption and diffusion in microporous materials [29,30], only a relatively small number of such models actually satisfy detailed balance and can therefore be properly referred to as *equilibrium* CA. This is because, in models which evolve through a non-Newtonian dynamics, the full synchronicity in the configurational update and the microscopic reversibility appear as two conflicting counterparts.

We recently developed a fully synchronous CA rule for adsorption and diffusion of mutually exclusive, locally interacting particles in a lattice which satisfies detailed balance [31,32]. So, as Little's model [33–35] represents the CA counterpart of the Ising model, the CA developed in Ref. [32] can be taken as the synchronous counterpart of the Kawasaki dynamics. Therefore, we refer to the evolution rule of our CA as "parallel Kawasaki" (PK).

This paper is devoted to the analytical derivation of the adsorption isotherm for a homogeneous, one-dimensional PK lattice. One-dimensional discrete models are of interest in the study of low-dimensional systems like, for example, single walled carbon nanotubes filled with molecules or atoms whose radius compared to the nanotube section is such that they cannot cross each other [36–39] and zeolite channels (see, for example, Refs. [40,41] and references therein).

This article is organized as follows: In Sec. II we summarize the PK evolution rule and pseudo-Hamiltonian. In Sec. III we develop a third-order finite difference equation for the grand-canonical partition function, from which we obtain an analytical relation between the density and the chemical

potential, and we discuss the effect of finite size of the lattice in Sec. IV. Finally, in Sec. V we compare the exact isotherms with two approximate models. Mathematical details are provided in the Appendix.

II. DESCRIPTION OF THE RULE

The characteristic parameters of the homogeneous PK model are [32] the site connectivity ν (i.e., the number of neighbors that can be accessed from each site), the site adsorption energy ε (with $\varepsilon \leqslant 0$), the site-to-site energy migration barrier ψ (with $\psi \geqslant 0$), and the interaction (dimensionless) parameter between a particle and an occupied neighboring site ϕ (with $0 \leqslant \phi < \infty$). In this work we incorporate a further interaction parameter, θ (with $\theta \geqslant 0$), describing the interaction between a particle and each *empty* site in its neighborhood. The condition $\theta = 1$ does not alter the tendency of a particle to point toward empty neighbors. If this is the case, then such tendency is determined only indirectly *via* the parameter ϕ (the parameter ϕ modifies the tendency to point toward filled neighboring sites and as a consequence modifies the tendency to point to the empty ones as well). Putting $\theta > 1$ emphasizes the tendency to point toward empty sites; i.e., it emphasizes *indirectly* the particle-particle repulsion, whereas $0 < \theta < 1$ suppresses the tendency to point to empty sites and as a consequence emphasizes the attraction among neighboring particles. The introduction of θ enlarges the parameter space of the model, thus enriching the range of possible behaviors of the system. This can be proven as follows. As we will show in the part of this work devoted to the equilibrium distribution of the model, a term which enters the expression for the interaction field around a particle is

$$F(\phi, \theta, N_r) = \nu\theta - N_r(\theta - \phi), \tag{1}$$

where N_r is the number of occupied neighboring sites around a particle located in site r. It is straightforward to check that, apart from the trivial case $\phi = \theta = 1$, it is not possible to define a ϕ' such that $F(\phi', 1, N_r) = F(\phi, \theta, N_r)$ without introducing an explicit dependence of ϕ' on the neighborhood occupancy N_r. In other words, there is no PK system with $\theta = 1$ whose properties are equivalent to a reference PK system with $\theta \neq 1$.

_____
[*]Corresponding author: fpazzona@uniss.it

This will become very clear in Sec. III, where we will show the effects on the adsorption isotherms caused by $\theta \neq 1$.

It is useful at this point to briefly summarize the PK evolution rule for a homogeneous lattice when we incorporate the parameter θ in the algorithm. Detailed balance is obeyed in the PK dynamics (PKD) by means of the following three prescriptions: (1) Empty sites can be pointed toward and reached by a particle in a neighboring site, whereas occupied sites can be pointed toward but cannot be reached; (2) if two or more particles are competing to occupy the same site, none of them will be allowed to reach it; and (3) if one of more particles are pointing toward a site occupied by another particle, that particle must stay at rest. Details about the the physical implications of such prescriptions can be found in Ref. [31].

We shall now define the neighborhood of each site, along with the probability each particle has to attempt a jump into a neighboring site. Let us indicate as r a generic site of the lattice $\mathcal{L}$. The ν sites connected to every site, say r, are listed in the set $\mathcal{I}(r)$, and they are called *neighbors of r*. The probability of a *lone* particle, located in the site r, to attempt a jump into site r' is defined as

$$p(r,r') = \frac{e^{\beta(\varepsilon-\psi)}}{\nu}, \quad r \neq r', \tag{2}$$

which is nonzero only for $r' \in \mathcal{I}(r)$. In Eq. (2), $\beta = (k_B T)^{-1}$ with k_B as the Boltzmann constant and T as the temperature, and $p(r,r') \leqslant 1$ because $\varepsilon \leqslant 0$ and $\psi \geqslant 0$. The probability of the host site itself, namely, r, to be chosen as the destination site reads consequently

$$p(r,r) = 1 - \sum_{r' \in \mathcal{I}(r)} p(r,r'). \tag{3}$$

Now, let us suppose that the presence of other particles in the neighborhood of a particle in r alters the probability of the particle in r to point toward each one of the sites in its neighborhood. More specifically, we assume such probability to be no longer $p(r,r')$ but $\tilde{p}(r,r')$ instead (called *direction probability*), defined as

$$\tilde{p}(r,r'|\boldsymbol{\eta}(r)) = \frac{p(r,r')}{Z(r,\boldsymbol{\eta}(r))}[\overline{n}(r')\theta + n(r')\phi], \tag{4}$$

valid for $r \neq r'$, and

$$\tilde{p}(r,r|\boldsymbol{\eta}(r)) = \frac{p(r,r)}{Z(r,\boldsymbol{\eta}(r))}, \tag{5}$$

for the case $r = r'$, where $n(r)$ represents the *occupancy* of site r (taking value 1 if r is occupied and zero otherwise), $\overline{n}(r)$ means $1 - n(r)$, and $\boldsymbol{\eta}(r) = \bigcup_{r' \in \mathcal{I}(r)} n(r')$ is the configuration of the occupancies in the neighborhood of site r (the occupancy of site r itself is excluded in this definition). In Eq. (4) the tendency of the particle in r to point toward site r' is modified either by the dimensionless parameter $\phi \geqslant 0$ if r' is filled or by $\theta > 0$ if r' is empty instead. This defines the interaction between a particle and its neighboring sites. The denominator $Z(r,\boldsymbol{\eta}(r))$ in Eq. (4) is defined as

$$Z(r,\boldsymbol{\eta}(r)) = p(r,r) + \sum_{r' \in \mathcal{I}(r)} p(r,r')[\overline{n}(r')\theta + n(r')\phi] \tag{6}$$

and is a key quantity since it represents the *local probability space* available to the particle located in r. The interaction parameters ϕ and θ modify the probability of particle i to escape its current host site. Repulsive and attractive effects can be obtained in several ways. For example, a mutually repulsive effect among neighboring particles can be obtained by setting $0 \leqslant \phi < 1$ and $\theta > 1$, and attraction can be mimicked by reverting those ranges. Setting $\phi = 1$ and $\theta = 1$ will mimic a situation of noninteraction (except mutual exclusion, which is ensured by the evolution algorithm).

Once we have defined all the basic quantities, we are ready to express mathematically the evolution rule according to prescriptions 1–3.

At each time step, at every site (independently of the other sites), say r, whose neighborhood occupancies are configured as $\boldsymbol{\eta}(r)$, we pick a random boolean $\xi(r,r')$ [with $r' \in \mathcal{I}(r)$] which is 1 with probability $\overline{p}(r,r'|\boldsymbol{\eta}(r))$ and zero otherwise. Note that $\xi(r,r) + \sum_{r' \in \mathcal{I}(r)} \xi(r,r') = 1$, so that every particle can choose only one target site at a time. The evolution rule for the site occupancies reads

$$n^{t+\tau}(r) - n^t(r) = \omega_{+1}(r)\overline{n^t}(r) - \omega_{-1}(r)n^t(r), \tag{7}$$

where t is the discrete time ($t = 0, \tau, 2\tau, \dots$) and τ is the duration (in s) of a time step. The quantities ω_{+1} and ω_{-1} in Eq. (7) are, respectively, creation and annihilation operators acting simultaneously on every lattice site. They are described in detail in Ref. [31].

We can follow the same method as in Ref. [32] to find out that the equilibrium configuration of occupancies satisfies

$$P(\boldsymbol{\eta}) \propto \prod_{r \in \mathcal{L}} [e^{-\beta\varepsilon} Z(r,\boldsymbol{\eta}(r))]^{n(r)}. \tag{8}$$

If we put the right-hand side of relation (8) in the form of $e^{-\beta\mathcal{H}_\beta(\boldsymbol{\eta})}$, where $\mathcal{H}_\beta(\boldsymbol{\eta})$ is the configurational pseudo-Hamiltonian, we get

$$\mathcal{H}_\beta(\boldsymbol{\eta}) = N\varepsilon - \frac{1}{\beta} \sum_r n(r) \ln \left\{ e^{-\beta\varepsilon} - \frac{e^{-\beta\psi}}{\nu} \right.$$
$$\left. \times \sum_{r' \in \mathcal{I}(r)} [1 - \theta + (\theta - \phi)n(r')] \right\}. \tag{9}$$

The inner summatory in the right-hand side of Eq. (9) is equivalent to $\nu - F(\phi,\theta,N_r)$, where the function F has been defined in Eq. (1). We remark that, since the sum in the definition of the direction probability, Eqs. (6) and (4), runs over the neighbors that can be reached with a single jump, and since the equilibrium distribution does not contain information about any extra interaction besides the neighboring interactions, in its present form the algorithm satisfies detailed balance if and only if every particle is allowed to attempt a jump from its current site to any of the sites it interacts with.

III. EXACT SOLUTION FOR A ONE-DIMENSIONAL SYSTEM

In this section we present the key points in the derivation of the exact expression for the adsorption isotherm of the PK model. Further details can be found in the Appendix.

Let us consider a one-dimensional PK lattice $\mathcal{L} := 1, \ldots, L$ of L sites. No periodic boundary conditions are assumed to hold; i.e., two sites, zero and $L+1$, are added, respectively, at the left of site 1 and at the right of site L and are assumed to remain always empty. The aim of this section is to obtain a recurrence equation [42] for the grand-canonical partition function

$$\Xi_L = \sum_{N=0}^{L} \lambda^N W_{N,L}, \qquad (10)$$

where $\lambda = e^{\beta(\mu-\varepsilon)}$ with μ as the chemical potential and ε as the site adsorption energy (assumed homogeneous); N is the number of particles in the lattice; and the weight $W_{N,L}$ contains the contributions of the particle-particle interactions to the total canonical partition function, $Q_{N,L} = W_{N,L}e^{-\beta\varepsilon N}$, when the number of particles and the number of sites have the values N and L, respectively. The weight $W_{N,L}$ (its definition can be found in the Appendix) contains three-body interactions of the form

$$Z(n_{i-1},n_i,n_{i+1}) = 1 - \frac{e^{\beta(\varepsilon-\psi)}}{\nu}[\nu(1-\theta) \\ + (n_{i-1}+n_{i+1})(\theta-\phi)]^{n_i}, \quad (11)$$

where the barriers ψ, θ, and ϕ are homogeneous throughout the entire lattice and $\nu = 2$ for a one-dimensional system. Equation (11) represents the statistical weight of the three-body interaction involving the ith site (with occupancy n_i) and its two neighboring sites, $i-1$ and $i+1$. We see immediately from Eq. (11) that the many-body nature of the PK interactions does not allow us to apply directly the formulas of Aranovich *et al.* [42], derived for the case of pair interactions. In PK lattices the energy of a pair of interacting particles depends on the state of the neighborhoods of both of them and cannot be reduced to a sum of pair interactions. We anticipate that this will raise the order of the resulting difference equation for Ξ from 2 [42] (the pair interaction case) to 3. Through combinatorial arguments [42,43], in the Appendix we derive a recurrence equation for $W_{N,L}$:

$$W_{N,L+1} - W_{N,L} - (1-y-2x)W_{N-1,L} - 2xW_{N-1,L-1} \\ - x^2 W_{N-2,L-2} = 0, \qquad (12)$$

where

$$y = e^{\beta(\varepsilon-\psi)}(1-\theta), \qquad x = \frac{e^{\beta(\varepsilon-\psi)}}{\nu}(\theta-\phi). \quad (13)$$

To retrieve an ordinary difference equation in terms of the grand-canonical partition functions Ξ_L, we simply multiply Eq. (12) by λ^N and then sum all the terms over $N = 0, \ldots, L+1$. Since $W_{N,L} = 0$ for $N < 0$ and $N > L$, by using Eq. (10) we get

$$\Xi_{L+1} - [1+\lambda(1-y-2x)]\Xi_L - 2\lambda x \Xi_{L-1} \\ - \lambda^2 x^2 \Xi_{L-2} = 0. \qquad (14)$$

Equation (14) is a third-order ordinary homogeneous difference equation, with general solution

$$\Xi_L = C_1\omega_1^L + C_2\omega_2^L + C_3\omega_3^L, \qquad (15)$$

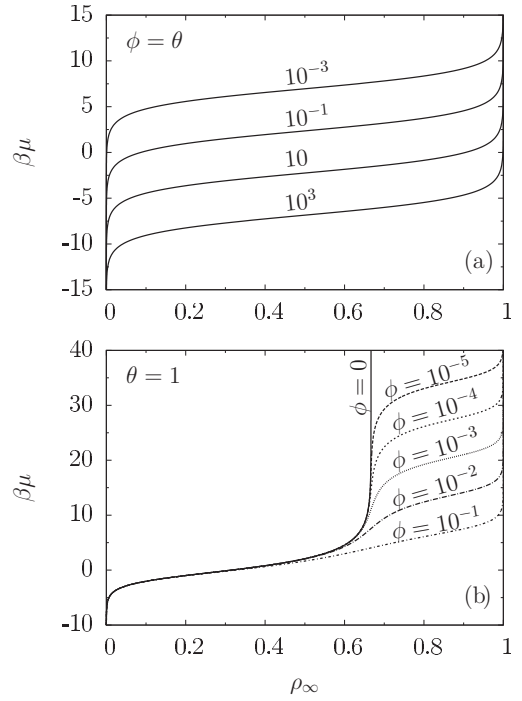FIG. 1. Adsorption isotherms ($T = 300$ K) for the one-dimensional PK lattice with null adsorption energy ε when (a) $\theta = \phi$, and when (b) the particle-particle attraction parameter ϕ is varied with $\theta = 1$.

where the functions C_k and ω_k ($k = 1,2,3$) do not depend on L. In particular, in the limit of $L \to \infty$ we have

$$\rho_\infty = 2\lambda\left\{1 - y - 2x + \frac{2^{4/3}[1-y+x+\lambda(1-y-2x)^2]}{(B_0+3\sqrt{3}B_1)^{1/3}} \right. \\ \left. - \frac{2^{4/3}B_3B_2}{(B_0+3\sqrt{3}B_1)^{4/3}} + \frac{2^{2/3}B_2}{(B_0+3\sqrt{3}B_1)^{2/3}}\right\} \Big/ \\ \left\{2[1+\lambda(1-y-2x)] + \frac{2^{4/3}B_3}{(B_0+3\sqrt{3}B_1)^{1/3}} \right. \\ \left. + 2^{2/3}(B_0+3\sqrt{3}B_1)^{1/3}\right\}. \qquad (16)$$

All the functions C_k, ω_k, and B_k are reported in the Appendix.

The expression in the right-hand side of Eq. (16) is quite complicated and is not amenable to immediate physical interpretation. We can, however, study Eq. (16) numerically. Since our aim is to study how the adsorption profiles change when we change the value of the interaction parameters θ and ϕ, in all the numerical examples we will consider $\varepsilon = \psi = 0$. Moreover, the temperature is fixed at the arbitrary value of 300 K.

If $\theta = \phi = 1$, the inner sum in the right-hand side of Eq. (9) becomes zero, so that the particles interact with each other only via mutual exclusion and the model is equivalent to the one described in our previous work [31]. However, the above mentioned sum does not become zero if $\theta = \phi \neq 1$ and the isotherm is therefore expected to differ from the case of absence of explicit particle-particle interactions. This is shown in Fig. 1(a), where we report the dimensionless chemical

potential, $\beta\mu$, necessary to reach every possible loading, ρ_∞, for an infinitely large one-dimensional system when equal values are assigned to the parameters θ and ϕ (the numerical values are reported above each curve). As we can see, a change in such a value induces a shift in the isotherm.

In Fig. 1(b) we set $\theta = 1$ and study the behavior of the isotherm under several values of ϕ, ranging from a situation of extreme particle-particle repulsion ($\phi = 0$) to one of modest repulsion ($\phi = 10^{-1}$). In the case of infinite repulsion ($\phi = 0$), an infinite step in the chemical potential prevents the infinite one-dimensional system from being loaded more than 2/3. This is because the infinite repulsion sets up (i.e., the energy diverges) when both the neighbors of a particle are occupied, whereas in the case of a single occupied neighbor the energy is still finite. Therefore, in the one-dimensional PK model a particle is not allowed to have two occupied neighbors if $\phi = 0$, and this causes an infinitely large μ step to appear at $\rho_\infty = 2/3$. For small (but non-null) values of ϕ the μ step becomes finite, indicating that a finite (but high) amount of energy must be supplied to load the system more than 2/3. This happens because the energy of a particle tends to become very high when both of its neighbors are occupied. Analogous steps have been observed in the adsorption isotherm of several experimental systems [44–47] and might indicate the presence of a liquid-solid phase transition (which in the standard Kawasaki is located at $\rho_c = 1/2$ rather than 2/3), but their nature is not clearly understood [42].

We remark that the infinite repulsion scenario is produced by $\phi = 0$ as well as by $\theta \to \infty$ and that the limiting case of an infinite chemical potential at $\rho_\infty = 2/3$ exists only when $\varepsilon = 0$. For ε slightly less than zero the infinite chemical potential barrier at $\rho_\infty = 2/3$ becomes a finite step, and as ε departs from zero to lower values the step tends to become less steep and finally disappears with a trend comparable with the one shown in Fig. 1(b) [32].

In Fig. 2 we show how the adsorption isotherm varies with both θ and ϕ. In Fig. 2(a) the extreme repulsion situation dictated by $\phi = 0$ forces the system to be loaded by 2/3 at most, and increasing the parameter θ from very low values (10^{-5}) to higher values (10^3) causes the chemical potential profile to be shifted to lower energies, which is compatible with the interpretation of θ as a parameter to model the affinity between particles and empty sites. In Fig. 2(b), the parameter ϕ is still low (10^{-5}) so a step around loading 2/3 is expected. However, the step does not appear until θ becomes several orders of magnitude larger than ϕ. This can be seen clearly in Figs. 2(b) and 2(c): the μ step does not exist at all when $\theta = \phi$, an inflection appears at $\theta = 10^{-3}$ (i.e., when $\theta = 10^2\phi$), a small step appears at $\theta = 10^{-1}$ (i.e., when $\theta = 10^4\phi$), and it becomes larger when we further increase by several orders of magnitude the ratio θ/ϕ.

IV. FINITE SIZE EFFECTS

It is interesting to study how the isotherm behaves when $L < \infty$ and to compare such behavior with the case of a finite, standard one-dimensional Kawasaki lattice [42]. In particular, we want to check for the presence of substeps in the adsorption isotherm—such substeps can be found in the standard Kawasaki [42] as well as in a number of
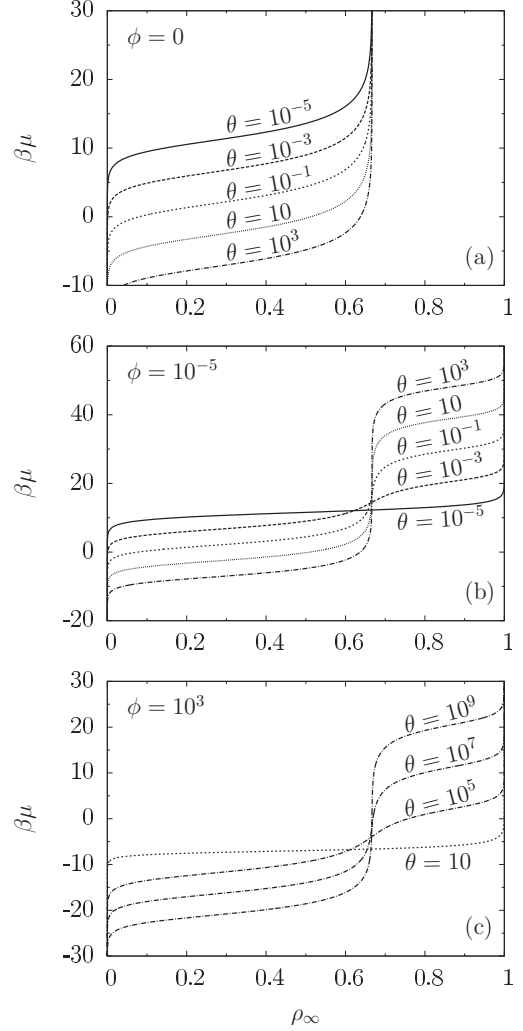

FIG. 2. Adsorption isotherms for the one-dimensional PK lattice with null adsorption energy ε for several values of the parameters θ and ϕ. Temperature is fixed at 300 K.

experimental systems [48,49]. The full explication of the grand-canonical partition function for a finite system, Ξ_L, through Eqs. (15), (A11)–(A18), and (A22)–(A24) in the relation $\partial \ln \Xi_L / \partial \ln \lambda$ provides a formula for ρ_L which is enormously more complicated than ρ_∞. Again, such exact solutions will be studied numerically. In Fig. 3 the effect of a finite value of L is shown in a case where a step in the adsorption isotherm is expected, i.e., $\theta = 1$ and $\phi = 10^{-5}$. In the standard Kawasaki case, substeps were likely to appear at even (and relatively small) values of L, i.e., with periodicity 2. Such a feature was strictly related to the fact that, for L even, a first substep was expected at $\rho_c = 1/2$, *plus* an additional substep was expected at $\rho_c = 1/2 + 1/N$ due to the fact that a further particle can be adsorbed either in the site at the end point of the lattice that has only one (rather than two) occupied neighbor or in any of the other sites of the lattice that has two occupied neighbors. The presence of substeps in the PK lattice can be explained in a similar manner. However, as one can see in Fig. 3, in the PK case oscillations appear for $L = 3k$ and $3k + 1$ ($k = 1, 2, \dots$).
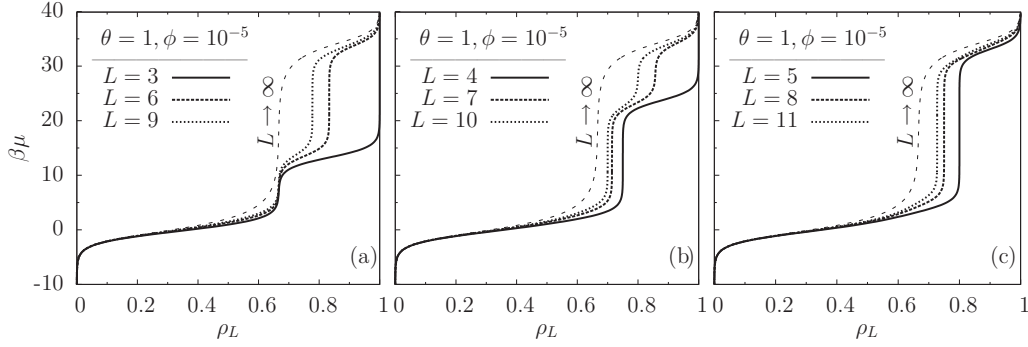
FIG. 3. Size effect on finite PK lattices with null adsorption energy ε. Temperature is fixed at 300 K.

More specifically, for the case of $L = 3k$ a first step occurs at $\rho_1 = N_1/L$ with $N_1 = 2Q(\frac{L}{3})$ [where $Q(\frac{A}{B})$ is the quotient between the integers A and B], corresponding to a configuration where $Q(\frac{L}{3})$ pairs of sites (separated by at least one empty site) are occupied. For example, for $L = 9$ such a configuration can be realized in one of the four ways

$$\blacksquare\blacksquare\square\blacksquare\blacksquare\square\blacksquare\blacksquare\square \tag{17}$$

$$\blacksquare\blacksquare\square\blacksquare\blacksquare\square\square\blacksquare\blacksquare \tag{18}$$

$$\blacksquare\blacksquare\square\square\blacksquare\blacksquare\square\blacksquare\blacksquare \tag{19}$$

$$\square\blacksquare\blacksquare\square\blacksquare\blacksquare\square\blacksquare\blacksquare \tag{20}$$

or in one of the six ways

$$\blacksquare\blacksquare\square\blacksquare\blacksquare\square\blacksquare\square\blacksquare \tag{21}$$

$$\blacksquare\blacksquare\square\blacksquare\square\blacksquare\blacksquare\square\blacksquare \tag{22}$$

$$\blacksquare\blacksquare\square\blacksquare\square\blacksquare\square\blacksquare\blacksquare \tag{23}$$

$$\blacksquare\square\blacksquare\blacksquare\square\blacksquare\square\blacksquare\blacksquare \tag{24}$$

$$\blacksquare\square\blacksquare\blacksquare\square\blacksquare\blacksquare\square\blacksquare \tag{25}$$

$$\blacksquare\square\blacksquare\square\blacksquare\blacksquare\square\blacksquare\blacksquare \tag{26}$$

In configurations (17)–(26) two kinds of clusters can be observed: clusters made of one site only (one-site clusters or clusters of order 1) and clusters made of two consecutive sites (two-site clusters or clusters of order 2). If w (with $w = 1, 2, \dots$) indicates the order of a cluster, and E_w indicates the energy of a w-site cluster calculated at the same conditions as in Fig. 3 (i.e., $\varepsilon = \psi = 0$, $\theta = 1$, and $\phi = 10^{-5}$), we have

$$\beta E_1 \approx 0.693, \quad \beta E_2 \approx 1.386. \tag{27}$$

The addition of one particle results in three kinds of clusters. Three-site clusters are obtained, e.g., by insertion in the ninth site of configuration (17) or in the seventh site of configuration

(18), resulting in

$$\blacksquare\blacksquare\square\blacksquare\blacksquare\square\underbrace{\blacksquare\blacksquare\blacksquare}_{w=3} \tag{28}$$

Four-site clusters are obtained, e.g., by inserting a particle in the third site of configuration (22):

$$\underbrace{\blacksquare\blacksquare\blacksquare\blacksquare}_{w=4}\square\blacksquare\blacksquare\square\blacksquare \tag{29}$$

Five-site clusters are obtained, e.g., by inserting a particle in the third site of configuration (17):

$$\underbrace{\blacksquare\blacksquare\blacksquare\blacksquare\blacksquare}_{w=5}\square\blacksquare\blacksquare\square \tag{30}$$

The energies E_3, E_4, and E_5 are one order of magnitude higher than E_1 and E_2:

$$\beta E_3 \approx 12.899, \quad \beta E_4 \approx 24.412, \quad \beta E_5 \approx 35.925. \tag{31}$$

To get from N_1 to $N_2 = 2Q(\frac{L}{3}) + 1$ particles, the energy spent to accommodate one further particle is at least the one necessary to the formation of a three-site cluster, resulting in the transition at the density

$$\rho_{3k}^{(1)} = \frac{2Q\left(\frac{L}{3}\right)}{L}. \tag{32}$$

An alternative route proceeds through the formation of a four-site cluster and is not preferred due to the greater amount of energy required. After the addition $N_1 \rightarrow N_1 + 1$, all the lattice sites that remained empty have equivalent energy, and thus at the density

$$\rho_{3k}^{(2)} = \frac{2Q\left(\frac{L}{3}\right) + 1}{L} \tag{33}$$

we have another transition to saturation, which is steeper than the previous one. Such behavior is expected, since the energy required for the addition $N_1 + 1 \rightarrow N_1 + 2$ is more than doubled with respect to the amount necessary for $N_1 \rightarrow N_1 + 1$. For example, addition of one particle into the empty end point of configuration (17) [which leads to configuration (28), made of two clusters of order 2 and one of order 3] takes $\beta\Delta E \approx 11.513$, and addition to a further particle into the third empty site of configuration (28) [leading to one cluster of order 5 and one of order 3] requires $\beta\Delta E \approx 33.153$.

For the case of $L = 3k + 1$ we have two steps at the densities

$$\rho_{3k+1}^{(1)} = \frac{2Q\left(\frac{L}{3}\right) + R\left(\frac{L}{3}\right)}{L} = 1 - \frac{Q\left(\frac{L}{3}\right)}{L} \tag{34}$$

and

$$\rho_{3k+1}^{(2)} = 1 - \frac{Q\left(\frac{L}{3}\right)}{L} + \frac{1}{L}, \tag{35}$$

where $R\left(\frac{A}{B}\right) = A - BQ\left(\frac{A}{B}\right)$ indicates the remainder of the division between the integers A and B. At the density $\rho_{3k+1}^{(1)}$ the most stable configuration is made of $Q\left(\frac{L}{3}\right)$ pairs and an isolated particle. An example for $L = 10$ is

$$\blacksquare\blacksquare\square\blacksquare\blacksquare\square\blacksquare\blacksquare\square\blacksquare \tag{36}$$

The particle addition which involves the minimum amount of energy is the addition into the ninth site, leading to a four-site cluster. In this case we do not have an alternative route allowing us to form a (less expensive) three-site cluster instead of a four-site one, and therefore the transition at the density $\rho_{3k+1}^{(1)}$ is expected to be the steepest one in this case.

The case of $L = 3k + 2$ is analogous to the case with an odd number of lattice sites in the ordinary Kawasaki algorithm. A unique transition point is located at the density

$$\rho_{3k+2}^{(1)} = 1 - \frac{Q\left(\frac{L}{3}\right)}{L}, \tag{37}$$

where the most stable configuration is made of only pairs, with no empty end points. For example, for $L = 11$ we have

$$\blacksquare\blacksquare\square\blacksquare\blacksquare\square\blacksquare\blacksquare\square\blacksquare\blacksquare \tag{38}$$

The empty sites are all equivalent and we have a single step in the adsorption isotherm.

V. APPROXIMATE SOLUTIONS

We checked the agreement between exact isotherms and the ones produced under two of the most widely used approximate solutions in lattice-gas theory, namely, the Bragg-Williams (BW) and the Bethe-Peierls (BP) approximations. Under the BW approximation [50], we have

$$\beta\mu = \beta\varepsilon - \frac{e^{\beta(\varepsilon-\psi)}\rho(\phi-\theta)}{1 + e^{\beta(\varepsilon-\psi)}[\theta - 1 + (\phi - \theta)\rho]} + \ln\frac{\rho}{1-\rho}$$
$$- \ln\{1 + e^{\beta(\varepsilon-\psi)}[\theta - 1 + (\phi - \theta)\rho]\}, \tag{39}$$

whereas under the BP approximation [51] we construct the isotherm by solving numerically, for every value of the chemical potential μ, the set of equations

$$P(1,n) = \frac{1}{q}\binom{\nu}{n}e^{\beta\mu(n+1)}z^n e^{-\beta\varepsilon}$$
$$\times \left\{1 - \frac{e^{\beta(\varepsilon-\psi)}}{\nu}[\nu(1-\theta) + n(\theta - \phi)]\right\},$$
$$P(0,n) = \frac{1}{q}\binom{\nu}{n}e^{\beta\mu n}z^n, \tag{40}$$

and

$$\sum_{n=0}^{\nu} P(1,n) = \frac{1}{\nu}\sum_{n=0}^{\nu} n\left[P(0,n) + P(1,n)\right]. \tag{41}$$

where $P(1,n)$ and $P(0,n)$ represent, respectively, the probability of a site to have n occupied neighbors when it is occupied or empty, ν still indicates the number of first neighbors and has value 2 for a one-dimensional system, z accounts for the influence of the rest of the lattice, and the factor q is obtained through the normalization condition

$$\sum_{n=0}^{\nu}[P(0,n) + P(1,n)] = 1. \tag{42}$$

Comparisons are made in Fig. 4. We notice immediately the qualitative inadequacy of the BW approximation for intermediate to high loadings, which mirrors the fact that no correlations between a site and its neighborhood are included in any way, so the difference between the exact
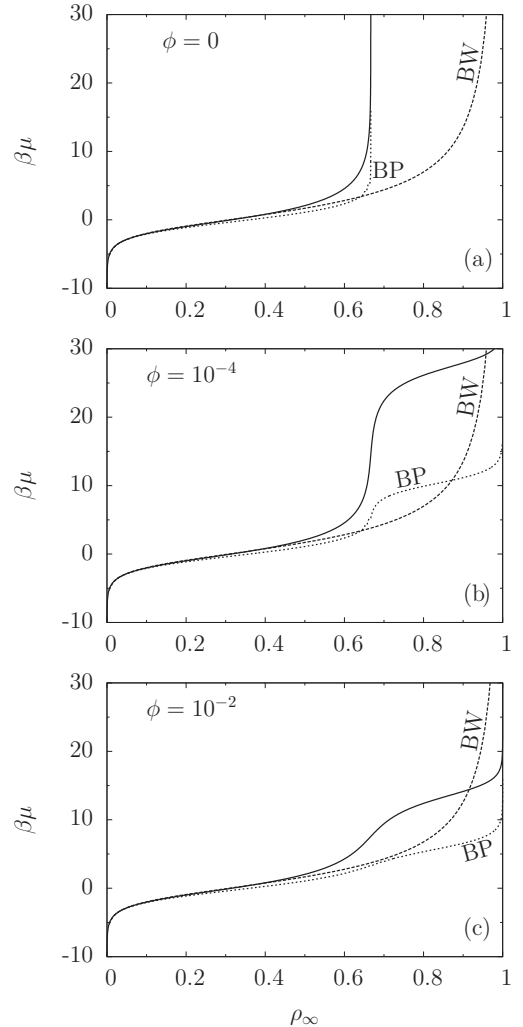

FIG. 4. Exact adsorption isotherms (solid lines) for the infinite PK model with $\theta = 1$, $T = 300$ K, and several values of ϕ, together with the curve resulting from both the Bragg-Williams (BW, dashed lines) and the Bethe-Peierls (BP, dotted lines) approximation.

and the BW isotherm can be taken as a measure of deviation from ideality. The qualitative agreement provided by the BP approximation instead can be considered satisfactory, since inflections are produced at the same critical loading as the exact isotherm, indicating that the very little information about correlations between the central site and the neighboring ones introduced in the BP equation [i.e., the term z in Eq. (40)] is enough for the approximate model to reproduce the behavior of the isotherm under highly nonideal conditions. Not surprisingly, the agreement is almost quantitative for the most extreme case, namely, $\phi = 0$. This is due to the presence in the approximate equations of the term $\{1 - \frac{e^{\beta(\varepsilon - \psi)}}{2}[2(1 - \theta) + n(\theta - \phi)]\}$ (with $n = 0, 1, 2$), which causes the pseudo-Hamiltonian to diverge when $\varepsilon = 0$ and $\psi = 0$.

VI. CONCLUSIONS

The present paper is aimed, on the one hand, to validate the simulation results presented in our previous work [32] and, on the other hand, to contribute to the still-ongoing production and study of one-dimensional lattice gases [52–55]. We derived a third-order finite difference equation for the grand-canonical partition function of the one-dimensional homogeneous parallel Kawasaki lattice gas. By solving it, we obtained analytical expressions for the adsorption isotherm when the interactions are represented through the dimensionless parameters ϕ, describing the tendency of a particle to point toward a neighboring filled site, and θ, which instead describes the tendency of a particle to point toward a neighboring *empty* site. The importance of $\theta \neq 1$ can be seen in the shift of the adsorption isotherms when $\theta = \phi$ and when $\phi = 0$ with $\theta \neq \phi$. We studied the solution for an infinite lattice and in particular the conditions leading to a step in the adsorption isotherm. Although it is common to observe steps in the isotherms of heterogeneous lattices [56,57], here the steps are purely related to situations of high particle-particle repulsion. We discussed the role of the lattice size in the production of further substeps in the adsorption isotherm, which are found to exist both in the standard Kawasaki model [42] and in several experimental systems [48,49]. Differently from the standard Kawasaki model, where the isotherm substeps belong to two categories depending on the loading at which they are observed, in our model the number of such categories is found to be 3. Finally, the qualitative validity of the Bethe-Peierls approximation is assessed in capturing the isotherm shape and reproducing the critical loading (in particular, the agreement is semiquantitative in the case of extreme repulsions), whereas the Bragg-Williams model turns out to be inadequate for all but the lowest loadings.

The range of possible applications of our model of adsorption covers the field of the theoretical treatment of problems related to adsorption and diffusion phenomena in one-dimensional nanochannels. The behavior of water adsorbed in materials like Na-ABW, Li-ABW, and bikitaite [58,59] as well as in AFI-type zeolites [60]; the use of EUO zeolites as hydrocarbon traps for the automobile exhaust cold-start problem [61]; and the properties of adsorbed molecules in the one-dimensional channels of zeolite L [62]

are some examples of systems that can be investigated through computational techniques, by means of molecular dynamics and Monte Carlo on the molecular scale and, in our opinion, by means of the PK model on the mesoscopic scale. Moreover, besides the analytically solved model presented here, which can cover the problem of adsorption in one-dimensional guest-host systems in which the guest is represented by one chemical species only, a great advantage of the PK model with respect to standard Kawasaki lattice-gas approaches is represented by its intrinsically synchronous nature, which makes it amenable to numerical implementation in parallel architectures, thus enabling the simulation of diffusion and adsorption properties on very large space and time scales.

APPENDIX: APPENDIX: DERIVATION OF THE ADSORPTION ISOTHERM

The statistical weight $W_{N,L}$ mentioned in Eq. (10) can be expressed as

$$W_{N,L} = \sum_{n_1,...,n_L}^{(N,L)} K_1^{L-1} Z(n_{L-1}, n_L, 0), \quad \text{(A1)}$$

where we introduced the notation

$$\sum_{n_1,...,n_L}^{(N,L)} = \sum_{n_1=0}^{1} \cdots \sum_{n_L=0}^{1} \delta\left(N - \sum_{i=1}^{L} n_i\right), \quad \text{(A2)}$$

and K_1^L is a shorthand notation for the product of all the local statistical weights from site 1 to site L:

$$K_1^L = Z(0, n_1, n_2) \left[\prod_{i=2}^{L-1} Z(n_{i-1}, n_i, n_{i+1})\right]. \quad \text{(A3)}$$

The function $Z(n_{i-1}, n_i, n_{i+1})$ is defined in Eq. (11). Since $n_i = 0 \vee 1$ (the same holds for n_{i-1} and n_{i+1} as well), it is convenient to rewrite Eq. (11) as

$$Z(n_{i-1}, n_i, n_{i+1}) = 1 - n_i y - n_i(n_{i-1} + n_{i+1})x, \quad \text{(A4)}$$

where x and y are defined in Eq. (13). Now, let us add a further site after site L, while keeping N constant, so that the N particles are now distributed over sites from 1 to $L+1$, with sites zero and $L+2$ *always empty*. We can divide the set of the possible configurations into two subsets where the site $L+1$ is empty and filled, respectively. In the configurations with empty $L+1$ all the N particles are distributed over sites 1 to L, and the partition function for this subset is again $W_{N,L}$. In the configurations with filled $L+1$, instead, there is one particle in the site $L+1$, and the remaining $N-1$ particles

are distributed over sites 1 to L. We will indicate the partition function of this subset as $W^*_{N-1,L}$, where the asterisk indicates that the Nth particle is always located at $L+1$:

$$
\begin{aligned}
W_{N,L+1} &= \sum_{n_1,\dots,n_{L+1}}^{(N,L+1)} K_1^{L-1} Z(n_{L-1},n_L,n_{L+1}) \\
&\quad \times Z(n_L,n_{L+1},0) \\
&= \sum_{n_1,\dots,n_L}^{(N,L)} K_1^{L-1} Z(n_{L-1},n_L,0) Z(n_L,0,0) \\
&\quad + \sum_{n_1,\dots,n_L}^{(N-1,L)} K_1^{L-1} Z(n_{L-1},n_L,1) Z(n_L,1,0) \\
&= W_{N,L} + W^*_{N-1,L},
\end{aligned}
\tag{A5}
$$

where we used the fact that $Z(n_L,0,0)=1$. In turn, the set of configurations over which $W^*_{N-1,L}$ is defined can be further divided into two subsets, one ($W^{**}_{N-2,L-1}$) with both the sites L and $L+1$ occupied and another one with L empty and $L+1$ occupied:

$$
\begin{aligned}
W^*_{N-1,L} &= \sum_{n_1,\dots,n_{L-1}}^{(N-2,L-1)} K_1^{L-2} Z(n_{L-2},n_{L-1},1) \\
&\quad \times Z(n_{L-1},1,1) Z(1,1,0) \\
&\quad + \sum_{n_1,\dots,n_{L-1}}^{(N-1,L-1)} K_1^{L-2} Z(n_{L-2},n_{L-1},0) \\
&\quad \times Z(n_{L-1},0,1) Z(0,1,0) \\
&= W^{**}_{N-2,L-1} + (1-y) W_{N-1,L-1},
\end{aligned}
\tag{A6}
$$

where we used $Z(n_{L-1},0,1)=1$ and $Z(0,1,0)=1-y$. Along with the same criterion the partition function $W^{**}_{N-2,L-1}$ can be further decomposed:

$$
\begin{aligned}
W^{**}_{N-2,L-1} &= \sum_{n_1,\dots,n_{L-2}}^{(N-2,L-2)} K_1^{L-3} Z(n_{L-3},n_{L-2},0) \\
&\quad \times Z(n_{L-2},0,1) Z(0,1,1) Z(1,1,0) \\
&\quad + \sum_{n_1,\dots,n_{L-2}}^{(N-3,L-2)} K_1^{L-3} Z(n_{L-3},n_{L-2},1) \\
&\quad \times Z(n_{L-2},1,1) Z(1,1,1) Z(1,1,0) \\
&= (1-y-x)^2 W_{N-2,L-2} \\
&\quad + (1-y-2x) W^{**}_{N-3,L-2},
\end{aligned}
\tag{A7}
$$

where we used $Z(n_{L-2},0,1)=1$, $Z(0,1,1)=Z(1,1,0)=1-x-y$, and $Z(1,1,1)=1-y-2x$. Now that we have found that $W_{N,L+1}$ can be expressed as

$$
W_{N,L+1} = W_{N,L} + (1-y) W_{N-1,L-1} + W^{**}_{N-2,L-1}, \tag{A8}
$$

we can lower the order of Eq. (A8) in both N and L to obtain

$$
W_{N-1,L} = W_{N-1,L-1} + (1-y) W_{N-2,L-2} + W^{**}_{N-3,L-2}, \tag{A9}
$$

that can be combined with Eqs. (A8) and (A7) to eliminate the terms $W^{**}_{N-2,L-1}$ and $W^{**}_{N-3,L-2}$, thus obtaining Eq. (12).

The ω_k in the right-hand side of Eq. (15) are the solutions to the third-degree equation

$$
\omega^3 - [1+\lambda(1-y-2x)]\omega^2 - 2\lambda x\omega - \lambda^2 x^2 = 0, \tag{A10}
$$

associated to Eq. (15), which has one real (ω_1) and two complex roots (ω_2, ω_3):

$$
\omega_1 = \tfrac{1}{6}(2G_1 + G_2 + G_3), \tag{A11}
$$

$$
\omega_2 = \frac{1}{12}(4G_1 - G_2 - G_3) + i\frac{\sqrt{3}}{12}(G_2 - G_3), \tag{A12}
$$

$$
\omega_3 = \frac{1}{12}(4G_1 - G_2 - G_3) - i\frac{\sqrt{3}}{12}(G_2 - G_3), \tag{A13}
$$

where G_1, G_2, and G_3 are functions of λ, x, and y:

$$
G_1 = 1 + \lambda(1-y-2x), \tag{A14}
$$

$$
G_2 = 2^{2/3}(B_0 + 3\sqrt{3}B_1)^{1/3}, \tag{A15}
$$

$$
G_3 = \frac{2^{4/3}[1 + 2\lambda(1-y+x) + \lambda^2(1-y-2x)^2]}{(B_0 + 3\sqrt{3}B_1)^{1/3}}. \tag{A16}
$$

In Eqs. (A14)–(A16) the quantities B_0 and B_1 read

$$
\begin{aligned}
B_0 &= 2 + 3\lambda^2[5x^2 - 2x(1-y) + 2(1-y)^2] \\
&\quad + 6\lambda(1-y+x) + 2\lambda^3(1-y-2x)^3,
\end{aligned}
\tag{A17}
$$

$$
\begin{aligned}
B_1 &= (\lambda^3 x^2 \{4\lambda^2(1-y-2x)^3 + 4(1-y-x) \\
&\quad - \lambda[13x^2 - 4x(1-y) - 8(1-y)^2]\})^{1/2}.
\end{aligned}
\tag{A18}
$$

Since Ξ_L is real, and since we have $\omega_2^* = \omega_3$, where $*$ denotes the conjugation operation, then we require also $C_2^* = C_3$. Therefore, by means of the boundary conditions

$$
\Xi_0 = 1, \tag{A19}
$$

$$
\Xi_1 = 1 + \lambda(1-y), \tag{A20}
$$

$$
\Xi_2 = 1 + 2\lambda(1-y) + \lambda^2(1-y-x)^2, \tag{A21}
$$

we can determine C_1, $\mathrm{Re}(C_2) = \mathrm{Re}(C_3)$, and $\mathrm{Im}(C_2) = -\mathrm{Im}(C_3)$, which read

$$
\begin{aligned}
C_1 &= \{4G_1^2 + G_2^2 - G_2 G_3 + G_3^2 + 6(G_2+G_3)\Xi_1 \\
&\quad - 2G_1(G_2 + G_3 + 12\Xi_1) \\
&\quad + 36\Xi_2\}/[3(G_2^2 + G_2 G_3 + G_3^2)],
\end{aligned}
\tag{A22}
$$

$$
\begin{aligned}
\mathrm{Re}(C_2) &= \{(G_2+G_3)(G_2+G_3-3\Xi_1) \\
&\quad + G_1(G_2+G_3+12\Xi_1) - 2G_1^2 \\
&\quad - 18\Xi_2\}/[3(G_2^2 + G_2 G_3 + G_3^2)],
\end{aligned}
\tag{A23}
$$

$$
\begin{aligned}
\mathrm{Im}(C_2) &= \{2G_1^2(G_2+G_3) - G_2^2(G_3+3\Xi_1) \\
&\quad - G_2(G_3^2 - 18\Xi_2) + G_1[G_2^2 + G_3(G_3 - 12\Xi_1) \\
&\quad - 12G_2\Xi_1] - 3G_3(G_3\Xi_1 - 6\Xi_2)\}/ \\
&\quad [\sqrt{3}(G_2^3 - G_3^3)].
\end{aligned}
\tag{A24}
$$

The general solution (15) can be differentiated with respect to λ to obtain an expression for the density, ρ_L. In the limit of $L \to \infty$ the solution ω_1 prevails, so that

$$\rho_\infty = \lim_{L \to \infty} \frac{1}{L} \frac{\partial \ln \Xi_L}{\partial \ln \lambda} = \frac{\partial \ln \omega_1}{\partial \ln \lambda}. \tag{A25}$$

By introducing the quantities B_2 and B_3 as

$$B_2 = 1 + x + \lambda[5x^2 - 2x(1-y) + 2(1-y)^2] - y + \lambda^2(1-y-2x)^3 - \frac{1}{B_1}(\sqrt{3}\lambda^2 x^2 \{\lambda[13x^2$$

$$- 4x(1-y) - 8(1-y)^2] - 3(1-x-y) - 5\lambda^2(1-y-2x)^3\}), \tag{A26}$$

$$B_3 = 1 + 2\lambda(1-y+x) + \lambda^2(1-y-2x)^2, \tag{A27}$$

we can write the formula in the right-hand side of Eq. (16).

---

[1] E. Ising, Z. Phys. **31**, 253 (1925).
[2] K. Kawasaki, Phys. Rev. **145**, 224 (1966).
[3] A. B. Bortz, M. H. Kalos, and J. L. Lebowitz, J. Comput. Phys. **17**, 10 (1975).
[4] H. C. Kang and W. H. Weinberg, J. Chem. Phys. **90**, 2824 (1989).
[5] Y. He and R. B. Pandey, Phys. Rev. Lett. **71**, 565 (1993).
[6] J. J. Alonso, J. Marro, and J. M. Gonzaléz-Miranda, Phys. Rev. E **47**, 885 (1993).
[7] Z. Zhang, Phys. Rev. E **51**, 4155 (1995).
[8] M. Hildebrand and A. S. Mikhailov, J. Phys. Chem. **100**, 19089 (1996).
[9] G. Giacomin and J. L. Lebowitz, J. Stat. Phys. **87**, 37 (1997).
[10] J. Marro and R. Dickman, *Nonequilibrium Phase Transitions in Lattice Models*, 1st ed. (Cambridge University Press, Cambridge, 1999).
[11] G. Franzese and H. E. Stanley, J. Phys.: Condens. Matter **14**, 2201 (2002).
[12] L. J. Dunne, G. Manos, and Z. Du, Chem. Phys. Lett. **377**, 551 (2003).
[13] P. Argyrakis, A. A. Chumak, and M. Maragakis, Phys. Rev. B **71**, 224304 (2005).
[14] P. Argyrakis, M. Maragakis, O. Chumak, and A. Zhugayevych, Phys. Rev. B **74**, 035418 (2006).
[15] P. Argyrakis, A. A. Chumak, and M. Maragakis, Phys. Rev. B **76**, 054209 (2007).
[16] S. H. Payne and H. J. Kreuzer, Phys. Rev. B **75**, 115403 (2007).
[17] R. Y. Guo and H. K. Huang, Physica (Utrecht) A **387**, 580 (2008).
[18] P. A. Monson, J. Chem. Phys. **128**, 084701 (2008).
[19] D. R. de Souza and T. Tomé, Physica (Utrecht) A **389**, 1142 (2010).
[20] G. L. Daquila and U. C. Täuber, Phys. Rev. E **83**, 051107 (2011).
[21] O. A. Pinto, F. Nieto, and A. J. Ramirez-Pastor, Phys. Rev. E **84**, 061142 (2011).
[22] R. Chen, Z. Chen, B. Ma, X. Hao, N. Kapur, J. Hyun, K. Cho, and B. Shan, Comput. Theor. Chem. **987**, 77 (2012).
[23] T. Becker, K. Nelissen, B. Cleuren, B. Partoens, and C. Van den Broeck, Phys. Rev. Lett. **111**, 110601 (2013).
[24] S. Wolfram, Rev. Modern Phys. **55**, 601 (1983).
[25] D. Dab, A. T. Lawniczak, J. P. Boon, and R. Kapral, Phys. Rev. Lett. **64**, 2462 (1990).
[26] J. P. Boon, D. Dab, R. Kapral, and A. T. Lawniczak, Phys. Rep. **273**, 55 (1996).
[27] B. Chopard and M. Droz, *Cellular Automata Modeling of Physical Systems*, 1st ed. (Cambridge University Press, Cambridge, 1998).
[28] J.-P. Rivet and J. P. Boon, *Lattice Gas Hydrodynamics*, 1st ed. (Cambridge University Press, Cambridge, 2001).
[29] F. G. Pazzona, P. Demontis, and G. B. Suffritti, J. Chem. Phys. **131**, 234703 (2009).
[30] F. G. Pazzona, P. Demontis, and G. B. Suffritti, J. Chem. Phys. **131**, 234704 (2009).
[31] F. G. Pazzona, P. Demontis, and G. B. Suffritti, Phys. Rev. E **87**, 063306 (2013).
[32] F. G. Pazzona, P. Demontis, and G. B. Suffritti, Phys. Rev. E **88**, 062114 (2013).
[33] W. A. Little, Math. Biosci. **19**, 101 (1974).
[34] P. Peretto, Biol. Cybern. **50**, 51 (1984).
[35] N. S. Skantzos and A. C. C. Coolen, J. Phys. A **33**, 1841 (2000).
[36] B. W. Smith, M. Monthioux, and D. E. Luzzi, Nature (London) **396**, 323 (1998).
[37] G. Stan and M. W. Cole, Surf. Sci. **395**, 280 (1998).
[38] M. Hodak and L. A. Girifalco, Phys. Rev. B **64**, 035407 (2001).
[39] M. Hodak and L. A. Girifalco, Phys. Rev. B **68**, 085405 (2003).
[40] P. Demontis and G. B. Suffritti, Phys. Rev. E **74**, 051112 (2006).
[41] S. Chatterjee and G. M. Schütz, Microporous Mesoporous Mater. **125**, 143 (2009).
[42] G. L. Aranovich, T. E. Wetzel, and M. D. Donohue, J. Phys. Chem. B **109**, 10189 (2005).
[43] J. L. Hock and R. B. McQuistan, J. Math. Phys. **26**, 2392 (1985).
[44] E. Maglara, A. Pullen, D. Sullivan, and W. C. Conner, Langmuir **10**, 4167 (1994).
[45] F. Villieras, R. Leboda, B. Charmas, F. Bardot, G. Gerard, and W. Rudzinski, Carbon **36**, 1501 (1998).
[46] Z. Ryu, J. Zheng, M. Wang, and B. Zhang, J. Colloid Interface Sci. **230**, 312 (2000).
[47] S. Villar-Rodil, R. Denoyel, J. Roquerol, A. Martinez-Alonso, and J. M. D. Tascon, J. Colloid Interface Sci. **252**, 169 (2002).

[48] L. D. Belyakova, A. M. Kalpakian, and A. V. Kiselev, Chromatographia **7**, 14 (1974).

[49] F. Roquerol, J. Roquerol, and K. Sing, *Adsorption by Powders and Porous Solids* (Academic, London, 1999).

[50] R. Salazar and L. D. Gelb, Phys. Rev. E **71**, 041502 (2005).

[51] K. Huang, *Statistical Mechanics* (Wiley, New York, 2000).

[52] M. B. Yilmaz, A. Rajagopal, and F. M. Zimmermann, Phys. Rev. B **69**, 125413 (2004).

[53] M. B. Yilmaz and F. M. Zimmermann, Phys. Rev. E **71**, 026127 (2005).

[54] D. A. Mirabella and C. M. Aldao, J. Stat. Mech. (2011) P03011.

[55] A. Fronczak, Phys. Rev. E **87**, 022131 (2013).

[56] Z. Chvoj, H. Conrad, V. Cháb, M. Ondrejcek, and A. M. Bradshaw, Surf. Sci. **329**, 121 (1995).

[57] Z. Chvoj, H. Conrad, and V. Cháb, Surf. Sci. **376**, 205 (1997).

[58] E. Fois, A. Gamba, G. Tabacchi, S. Quartieri, and G. Vezzalini, Phys. Chem. Chem. Phys. **3**, 4158 (2001).

[59] P. Demontis, G. Stara, and G. B. Suffritti, J. Chem. Phys. **120**, 9233 (2004).

[60] P. Demontis, J. Gulín-González, and G. B. Suffritti, J. Phys. Chem. C **116**, 11100 (2012).

[61] K. F. Czaplewski, T. L. Reitz, Y. J. Kim, and R. Q. Snurr, Microporous Mesoporous Mater. **56**, 55 (2002).

[62] M. Busby, A. Devaux, C. Blum, V. Subramaniam, G. Calzaferri, and L. De Cola, J. Phys. Chem. C **115**, 5974 (2011).